



**HAL**  
open science

# Multi-Variable and Multi-Objective Gain-Scheduled Control Based on Youla-Kucera Parameterization: Application to Autonomous Vehicles

Hussam Atoui, Olivier Sename, Vicente Milanés, John Jairo Martínez Molina

► **To cite this version:**

Hussam Atoui, Olivier Sename, Vicente Milanés, John Jairo Martínez Molina. Multi-Variable and Multi-Objective Gain-Scheduled Control Based on Youla-Kucera Parameterization: Application to Autonomous Vehicles. *International Journal of Robust and Nonlinear Control*, 2024, 34 (9), pp.5889-5909. 10.1002/rnc.7298 . hal-04511304

**HAL Id: hal-04511304**

**<https://hal.univ-grenoble-alpes.fr/hal-04511304>**

Submitted on 19 Mar 2024

**HAL** is a multi-disciplinary open access archive for the deposit and dissemination of scientific research documents, whether they are published or not. The documents may come from teaching and research institutions in France or abroad, or from public or private research centers.

L'archive ouverte pluridisciplinaire **HAL**, est destinée au dépôt et à la diffusion de documents scientifiques de niveau recherche, publiés ou non, émanant des établissements d'enseignement et de recherche français ou étrangers, des laboratoires publics ou privés.

**RESEARCH ARTICLE**

# Multi-Variable and Multi-Objective Gain-Scheduled Control Based on Youla-Kucera Parameterization: Application to Autonomous Vehicles

Hussam Atoui\*<sup>1,2</sup> | Olivier Sename<sup>2</sup> | Vicente Milanés<sup>3</sup> | John-Jairo Martínez-Molina<sup>2</sup>

<sup>1</sup>Research Department, Renault SAS,  
Guyancourt, France

<sup>2</sup>Control Department, Univ. Grenoble Alpes,  
CNRS, Grenoble INP, GIPSA-lab,  
Grenoble, France

<sup>3</sup>Spanish Engineering Division, Renault  
España SA, Valladolid, Spain

**Correspondence**

\*Hussam Atoui, 1 Avenue de Golf, 78280  
Guyancourt, France. Email:  
hussam.atoui@outlook.com

**Present Address**

1 Avenue de Golf, 78280 Guyancourt, France

**Abstract**

This paper presents a Youla-Kucera based interpolation between a set of Linear Parameter-Varying (LPV) controllers, each one being a gain-scheduled of Linear Time-Invariant (LTI) controllers designed separately for different operating points. The gain-scheduling is achieved based on Youla-Kucera (YK) parameterization. A generalized LPV-YK control structure is designed to interpolate between various LPV controllers. The closed-loop system is proved to guarantee the quadratic stability for any continuous/discontinuous interpolating signals in terms of a set of Linear Matrix Inequalities (LMIs). The proposed method can help multi-variable and multi-objective systems to achieve high performances at different operating conditions and different critical situations regardless of the interpolation rate. A numerical example is simulated to show the importance of the proposed method to achieve different objectives for lateral control of autonomous vehicles. In addition, the approach has been tested on a real Renault ZOE vehicle to validate its real performance, and compare it with a standard polytopic LPV controller.

**KEYWORDS:**

Youla Parameterization, LPV Control, Autonomous Vehicles, Multi-objective Systems

## 1 Introduction And Motivation

Nowadays, systems are getting more and more complex leading to control algorithms able to consider online varying objectives for performance and safety. The field of autonomous systems, in particular autonomous vehicles, is indicative of such an evolution. Indeed, their driving capabilities have been recently improved for highly, and even fully, autonomous driving thanks to advanced control theory. A fully autonomous car needs to perform several tasks including longitudinal control, lateral control, chassis control, etc. Moreover, the lateral dynamics of an autonomous vehicle varies significantly with respect to its longitudinal speed<sup>1, 2</sup>. Specifically, at low speeds, the lateral dynamics becomes harder to be controlled (due to approaching system singularity), whereas at high speeds, robustness and system stability decrease<sup>3</sup>. On the other hand, even at nominal speeds, the lateral control aims to achieve various objectives such as lane tracking, lane changing, obstacle avoidance, etc. Consequently, various performances are required accordingly for different traffic situations that faces the vehicle. However, it is difficult to design a single controller covering the full speed range and achieving multiple objectives. As shown below, some solutions have been investigated in the literature to design multi-variable and multi-objective controllers to obtain various closed-loop performances.

## 1.1 Gain-scheduling Control Systems

In the last decades, research studies have developed multi-variable control systems using gain-scheduling techniques, see for instance the pioneering works<sup>4, 5</sup>. Gain-scheduling controls are used when a plant changes significantly within its operating conditions; which is actually the case in many real applications, see<sup>6</sup> and references therein. For time-varying systems, it may not be possible to find a single Linear Time-Invariant (LTI) controller that can perform well for all operating conditions. Therefore, the Linear Parameter-Varying (LPV) control concept has been successfully developed to achieve a stable gain-scheduling<sup>7</sup>, self-scheduling<sup>8</sup> or interpolation<sup>9</sup> between LTI systems synthesized at different operating points.

Recent works have been investigated in the theory and application of LPV as shown in the books<sup>10, 11, 12</sup>, and surveys<sup>6, 13</sup>. LPV control design methods have been examined with successful control applications on autonomous vehicles, see for instance<sup>14, 15, 16, 17, 18, 19</sup> and references therein. Nonetheless, it is today admitted that designing a single LPV controller for a large number of parameters, and/or for a wide range of variations of parameters may be conservative<sup>20</sup>. Two main solutions could be used to decrease the optimization problem conservatism: 1) Divide the parameter region into small subregions and use multiple parameter-dependent Lyapunov functions<sup>20</sup>; and 2) Use the Youla-Kucera (YK) parameterization to interpolate between different LTI controllers designed separately at each operating condition<sup>21</sup>.

The interest behind YK concept is to parameterize a set of linear stabilizing controllers  $K(Q)$  where each one is parameterized by its corresponding YK parameter  $Q$ <sup>22</sup>. In<sup>23</sup>, a YK configuration is considered to improve the performance of a polytopic LPV control. It introduces an LPV system which switches between a minimum-phase and nonminimum-phase dynamics as a function of the parameter variations. An LPV controller based on the polytopic approach is designed as a nominal controller in the full parameter region. Then, two different LTI controllers ( $H_\infty$  and PID) are designed separately at certain operating conditions (one in minimum-phase region and another in nonminimum-phase region). These LTI controllers are then interpolated with the nominal LPV controller using an LTI-YK configuration.

On the other hand,<sup>21</sup> proposes a YK-based gain-scheduled controller by interpolating LTI controllers designed separately at the different vertices of a polytopic parameter region. The interpolation is performed as a function of the varying parameters of the LPV model. Closed-loop quadratic stability and performance are guaranteed at intermediate interpolation points of the convex domain. In<sup>24</sup>, a fixed pole-assignment application is introduced using an LPV YK-based method to preserve the closed-loop poles at the same location by interpolating between different controllers.

In<sup>25</sup> an observer-based state-feedback LPV controller is designed based on Youla parameterization. It is proved that any quadratically stabilizing LPV controller can be parameterized based on YK concept, providing the closed-loop quadratic stability. A parameter-varying YK parameter  $Q(\rho)$  is designed, being  $\rho$  a measurable varying parameter. Recently,<sup>26</sup> proposes two different LPV-YK control structures aiming to maintain a robust performance over a wide range of parameters variations. The objective is to partition the varying parameter region into multiple subsets, and design a distinct LPV controller over each subset. Then, an LPV-YK control structure is proposed to switch between the LPV controllers over the parameter subsets with guaranteeing the closed-loop stability.

## 1.2 Youla-Kucera for Multi-Objective Control Systems

In addition to parameter-varying control performance, it may be required to reach several performance specifications (high robustness, fast/slow response, noise rejection, etc.) at each operating condition of the varying parameter region. The YK configuration has been widely used to interpolate between different performances, however mainly for LTI systems. Hespanha and Morse<sup>27</sup> propose the YK concept to interpolate between two LTI controllers (slow and fast) to handle both noise rejection and fast tracking performances.

The YK parameterization for interpolating controllers has shown several advantages: 1) It allows stable interpolation between unstable controllers<sup>28</sup>; 2) Interpolated controllers can be designed and tuned separately using different techniques ( $H_\infty$ , LQR, PID, ...) <sup>29</sup>; 3) It facilitates adding new parts to an existing system online as Plug&Play control theory<sup>30</sup>; and 4) The closed-loop stability is guaranteed under arbitrary continuous/discontinuous interpolating signals between different stabilizing controllers without requiring a common Lyapunov function<sup>27</sup>.

Recently,<sup>31</sup> proposes a YK-based interpolation scheme between two LPV controllers, designed separately, to achieve a multi-objective control system. Each LPV controller is designed over a convex domain with a common Lyapunov function (following the approach in<sup>7</sup>), to quadratically stabilize the plant model. However, this approach may be conservative since it requires all the local LPV controllers to be designed based on standard polytopic-based LPV approach.

A significant literature review on YK work including applications can be found in<sup>32</sup>. The YK parameterization has been successfully used in several domains such as noise/vibration control<sup>33</sup>, and steering control of autonomous vehicles considering two LTI controllers designed separately (one for lane-changing and one for lane-tracking)<sup>34</sup>. The YK control scheme of both controllers has shown interesting performance for small and large lateral errors. On the other hand, the YK controller is parameterized for a fixed-speed (LTI lateral dynamics). Our paper proposes a generalized LPV-YK control structure that interpolates between multiple LPV controllers obtaining a multi-variable and multi-objective gain-scheduled controller.

### 1.3 Motivation and Contribution

Apart from the YK concept, there has been a wide range of research to develop an LPV switching controller (see for instance<sup>20, 35</sup>). Recent extensions have mainly aimed to decrease the design complexity and conservatism<sup>36</sup>, and to provide smooth switching<sup>37</sup>. However, the LPV switching studies are still conservative due to the re-design of the local LPV controllers by proposed LMIs, in addition to some limitations that restrict the switching signals (e.g. hysteresis switching, switching with average dwell-time, etc.). The current work proposes an LPV interpolation/switching control scheme with lower conservatism and without any limitation on the switching signals. A new survey about different LPV switching methods, including YK-based approach, is presented in<sup>38</sup>.

A main motivation behind considering an interpolation scheme between multiple LPV controllers is the application to autonomous vehicles. Several studies have involved the LPV control approaches to solve the lateral tracking problem over the full speed-range (speed as the varying parameter), such as LPV/LFT<sup>15</sup> and grid-based LPV<sup>16, 39</sup>. However, it is not sufficient to achieve several tracking performances (e.g. smooth and aggressive). On the other hand,<sup>34</sup> has integrated lane-tracking and lane-changing control performances at a constant speed using LTI-YK concept.

Our work proposes a generalized LPV-YK control configuration which can guarantee several control objectives over the full speed-range. The main contributions are as follows:

1. An interpolation scheme of multiple LPV controllers is designed based on YK concept. Such scheme is considered to be more efficient and less conservative than the LPV switching control systems where: 1) There is no limitation on the switching/interpolating signals; 2) The local LPV controllers are designed based on LTI-YK parameterized controllers; 3) All the local LPV and LTI controllers are pre-defined and designed separately without requiring any common condition or re-design.
2. A generalized LPV-YK interpolation scheme is defined and proved to achieve closed-loop quadratic stability with smooth assumptions and LMI conditions.
3. A significant simulation shows the importance of the proposed LPV-YK control structure in improving the performance of the autonomous vehicles in various tasks and critical situations.
4. For the first time, the LPV-YK control scheme is implemented on a real Renault ZOE vehicle. An experimental test on the vehicle lateral control enhances the stability of the closed-loop system at the interpolating time instants, and shows the different performances achieved by the vehicle.

As a result, an interpolation scheme is drawn between multi-LPV controllers based on YK parameterization which guarantees the closed-loop quadratic stability under arbitrary interpolating signal. Moreover, it shows high flexibility to achieve various performance levels, and to add or remove controllers from the interpolation scheme without repeating the design step.

The paper is organized as follows: Section 2 defines the YK concept with some Lemmas to be used throughout the paper. The problem statement is expressed in Section 3. Section 4 introduces the main results, including the quadratic stability analysis. Section 5 presents the implementation control scheme of the LPV-YK controller. Section 6 shows an application to the autonomous vehicle lateral control, including simulation results. Experimental results of a robotized Renault ZOE vehicle are depicted in Section 7. Finally, some concluding remarks are given in Section 8.

Notations in this paper are as follows.  $\mathbb{I}[a, b]$  denotes the integer set from  $a$  to  $b$ .  $\mathbb{R}$  stands for the set of real numbers.  $\mathbb{R}^{m \times n}$  is the set of real  $m \times n$  matrices. The transpose of a real matrix  $M$  is denoted by  $M^T$ .  $I$  and  $0$  denote an identity matrix and a zero matrix, respectively, of appropriate dimensions.  $diag(X_1, X_2, \dots, X_N)$  denotes a matrix with matrices  $X_1, X_2, \dots$ , and  $X_N$  as diagonal blocks. Define a vector  $\gamma = [\gamma_1 \dots \gamma_c]$ , we note by  $\gamma_c^* = 1$  if  $\gamma_c = 1$  and  $\gamma_j = 0 \forall j \neq c$ .

In the whole paper, the subscript  $i$  of a system/matrix/variable of an LPV system (e.g.  $G_i, A_i, w_i$ ) denotes the local LTI system/matrix/variable at the  $i^{\text{th}}$  vertex of a polytope  $\mathcal{P}$ . The superscript  $(j)$  denotes the  $j^{\text{th}}$  controller (e.g.  $K^{(j)}$ ) in the set of designed controllers. For example,  $A_{k,i}^{(j)}$  represents the state matrix of the  $j^{\text{th}}$  LTI local controller at the  $i^{\text{th}}$  vertex of  $\mathcal{P}$ .

## 2 Preliminaries

This section introduces some notations and assumptions regarding LPV systems and LTI-YK parameterization. In addition, useful concepts and several lemmas are reviewed.

### 2.1 State Transformation

The concept of state transformation is to evolve the states of a system without affecting its input/output property. Consider a state transformation matrix  $T$  which transforms the state of a dynamic system  $W$  with the state-space representation;  $W : \begin{bmatrix} A & B \\ C & D \end{bmatrix}$ . Then, the transformed system  $\bar{W}$  is computed as:

$$\bar{W} : \left[ \begin{array}{c|c} TAT^{-1} & TB \\ \hline CT^{-1} & D \end{array} \right]. \quad (1)$$

**Lemma 1.** Consider a set of matrices  $A_i$  corresponding to each vertex of a convex hull  $\mathcal{J} = \mathcal{C}_{\mathcal{O}}\{w_1, \dots, w_{2^{n_p}}\}$ , The following statements are equivalent:

- (i)  $A_i$  is Hurwitz  $\forall i \in \llbracket 1, 2^{n_p} \rrbracket$
- (ii) there exist  $2^{n_p}$  transformation matrices  $T_i$  such that the LPV matrix

$$\bar{A}(\rho) = \sum_{i=1}^{2^{n_p}} \alpha_i(\rho) \bar{A}_i = \sum_{i=1}^{2^{n_p}} \alpha_i(\rho) T_i A_i T_i^{-1} \quad (2)$$

is quadratically stable  $\forall \rho \in \mathcal{J}$ , where  $\rho = \sum_{i=1}^{2^{n_p}} \alpha_i(\rho) w_i$  such that  $\sum_{i=1}^{2^{n_p}} \alpha_i(\rho) = 1, \alpha_i(\rho) \geq 0 \forall i$ .

Proof details are in<sup>21</sup> and<sup>27</sup>.

### 2.2 Doubly Coprime Factorisation

YK parameterisation uses the doubly coprime factorisation concepts to reduce the algebraic complexity of  $Q$  computation<sup>40</sup>. Let  $K$  be an LTI controller that stabilizes the LTI plant  $G$ , then both of them can be factorized (from left and right) as a product of a stable transfer function matrix and a transfer function matrix with a stable inverse as shown below:

$$\begin{aligned} G &= NM^{-1} = \tilde{M}^{-1} \tilde{N} \\ K &= UV^{-1} = \tilde{V}^{-1} \tilde{U} \end{aligned} \quad (3)$$

**Lemma 2.** If the coprime factors  $M, N, \tilde{M}, \tilde{N}, U, V, \tilde{U}, \tilde{V} \in \mathcal{RH}_{\infty}$  (proper, stable and rational), and they satisfy the following *Bezout Identity*:

$$\begin{aligned} \begin{bmatrix} \tilde{V} & -\tilde{U} \\ -\tilde{N} & \tilde{M} \end{bmatrix} \begin{bmatrix} M & U \\ N & V \end{bmatrix} &= \begin{bmatrix} M & U \\ N & V \end{bmatrix} \begin{bmatrix} \tilde{V} & -\tilde{U} \\ -\tilde{N} & \tilde{M} \end{bmatrix} \\ &= \begin{bmatrix} I & 0 \\ 0 & I \end{bmatrix} \end{aligned} \quad (4)$$

then, the factorized LTI controller  $K = UV^{-1}$  stabilizes  $G$ <sup>29</sup>.

### 2.3 Interpolation of two LPV controllers based on LPV-YK parameterization

This section summarizes some results already presented by the authors in<sup>31</sup>. Assume a set of two LPV controllers  $\{K^{(0)}(\rho), K^{(1)}(\rho)\}$  that have been designed separately to quadratically stabilize an LPV plant  $G(\rho)$  over a convex parameter

region  $\mathcal{P}$  ( $\rho \in \mathcal{P}$ ). Let us choose  $K^{(0)}(\rho)$  as the nominal controller for YK parameterization. Denote the LPV-YK parameter  $Q^{(1)}(\rho)$  as a transfer function matrix which characterizes the dynamic variation between  $K^{(0)}(\rho)$  and its corresponding controller  $K^{(1)}(\rho)$ .

**Lemma 3.** Assume a factorized LPV plant  $G(\rho) = N(\rho)M^{-1}(\rho)$ , and factorized LPV controllers  $K^{(0)}(\rho) = U^{(0)}(\rho)(V^{(0)}(\rho))^{-1}$  and  $K^{(1)}(\rho) = U^{(1)}(\rho)(V^{(1)}(\rho))^{-1}$  that quadratically stabilize  $G(\rho)$  over  $\mathcal{P}$ , with  $M(\rho)$  and  $N(\rho)$  are parameter-varying, coprime and stable,  $U^{(0)}(\rho)$  and  $V^{(0)}(\rho)$ ,  $U^{(1)}(\rho)$  and  $V^{(1)}(\rho)$  are parameter-varying, coprime and stable. Choosing  $K^{(0)}(\rho)$  as the nominal controller, then, the interpolation between both LPV controllers  $K^{(0)}(\rho)$  and  $K^{(1)}(\rho)$  can be performed using the parameterized LPV-YK controller  $\tilde{K}^{(1)}(\rho, \gamma)$  defined as:

$$\begin{aligned} \tilde{K}^{(1)}(\rho, \gamma) &= \left( U^{(0)}(\rho) + M(\rho)\gamma Q^{(1)}(\rho) \right) \left( V^{(0)}(\rho) + N(\rho)\gamma Q^{(1)}(\rho) \right)^{-1} \\ &= \left( \tilde{V}^{(0)}(\rho) + \gamma Q^{(1)}(\rho)\tilde{N}(\rho) \right)^{-1} \left( \tilde{U}^{(0)}(\rho) + \gamma Q^{(1)}(\rho)\tilde{M}(\rho) \right) \end{aligned} \quad (5)$$

where  $\gamma \in [0, 1]$  is the interpolating signal. Notice that  $K^{(0)}(\rho)$  is the nominal controller for which its corresponding YK parameter  $Q^{(0)}(\rho) = 0$ . It is proved that for every continuous/discontinuous interpolating signal  $\gamma$ ,  $\tilde{K}^{(1)}(\rho, \gamma)$  quadratically stabilizes  $G(\rho)$ , see<sup>31</sup> for proof. The interpolation method is represented as follows:

- if  $\gamma = 0$ ,  $\tilde{K}^{(1)}(\rho, \gamma) \equiv K^{(0)}(\rho)$
- if  $\gamma = 1$ ,  $\tilde{K}^{(1)}(\rho, \gamma) \equiv K^{(1)}(\rho)$
- else,  $\tilde{K}^{(1)}(\rho, \gamma)$  represents the interpolation between both controllers  $K^{(0)}(\rho)$  and  $K^{(1)}(\rho)$  according to the chosen  $\gamma$ .

### 3 Problem Statement

This section defines the considered LPV system with its stabilizing controllers. In addition, it presents the definition of an interpolation between multiple LPV controllers including some assumptions.

#### 3.1 LPV Plant and Controllers Description

Consider a Multi-Input-Multi-Output (MIMO) LPV system  $G(\rho)$  with  $m$  inputs and  $p$  outputs:

$$G(\rho) \begin{cases} \dot{x}(t) = A(\rho(t))x(t) + B_1(\rho(t))w(t) + B_2(\rho(t))u(t) \\ z(t) = C_1(\rho(t))x(t) + D_{11}(\rho(t))w(t) + D_{12}(\rho(t))u(t) \\ y(t) = C_2(\rho(t))x(t) + D_{21}(\rho(t))w(t) + D_{22}(\rho(t))u(t) \end{cases} \quad (6)$$

where  $x(t) \in \mathbb{R}^{n_x}$ ,  $y(t) \in \mathbb{R}^p$ ,  $u(t) \in \mathbb{R}^m$ ,  $z(t) \in \mathbb{R}^{n_z}$  are the state, output, input, controlled output vectors respectively.  $w(t) = [r \ n \ d]^T \in \mathbb{R}^{n_w}$  contains the exogenous inputs of the tracking reference  $r$ , noise  $n$  and input disturbance  $d$ .  $\rho(t) := \rho \in \mathbb{R}^{n_p}$  is a vector of  $n_p$  measurable time-varying parameters.

An LPV system can be handled for control design purpose using different approaches<sup>6</sup>. The polytopic approach is chosen in this work, which requires two assumptions: 1) the system must be strictly proper ( $D_{22}(\rho) = 0$ ); and 2) the input and output matrices  $B_2$ ,  $C_2$ ,  $D_{12}$  and  $D_{21}$  must be parameter-independent<sup>41</sup>. From now on, we assume, without loss of generality, that the LPV system is given as:

$$G(\rho) \begin{cases} \dot{x}(t) = A(\rho)x(t) + B_1(\rho)w(t) + B_2u(t) \\ z(t) = C_1(\rho)x(t) + D_{11}(\rho)w(t) + D_{12}u(t) \\ y(t) = C_2x(t) + D_{21}w(t) \end{cases} \quad (7)$$

Notice that the second assumption does not impose any serious constraints since, if needed, it can be fulfilled by filtering the input  $u$  and output  $y$  (details are given in<sup>8</sup>). Here,  $\rho$  belongs to a convex polytopic region  $\mathcal{P}$  defined by the parameters extremums  $[\underline{\rho}, \bar{\rho}]$  as:

$$\mathcal{P} := C_{\mathcal{O}}\{w_1, \dots, w_{2^{n_p}}\} \quad (8)$$

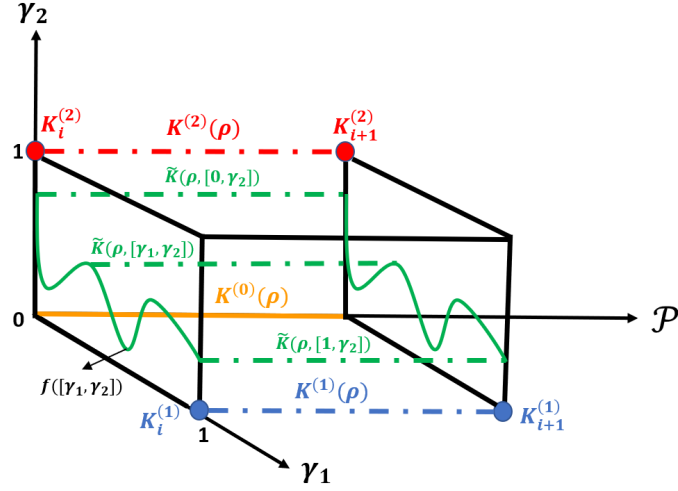


**FIGURE 1** Interpolation between three LPV controllers; two YK-based gain-scheduled controllers  $K^{(1)}(\rho)$  and  $K^{(2)}(\rho)$ , and a polytopic-based LPV controller  $K^{(0)}(\rho)$  along the convex parameter space  $\mathcal{P}$ . The LPV-YK controller  $\tilde{K}(\rho, \gamma)$  interpolates, using  $\gamma = [\gamma_1, \gamma_2]$ , between  $K^{(0)}(\rho)$  (for  $\gamma = [0, 0]$ ),  $K^{(1)}(\rho)$  (for  $\gamma = [1, 0]$ ), and  $K^{(2)}(\rho)$  (for  $\gamma = [0, 1]$ )

where  $w_i$  represent the vertices of  $\mathcal{P} \forall i \in \llbracket 1, 2^{n_p} \rrbracket$ .  $\rho$  is then scheduled as:

$$\rho = \sum_{i=1}^{2^{n_p}} \alpha_i w_i, \quad (9)$$

where  $\sum_{i=1}^{2^{n_p}} \alpha_i = 1$ ,  $\alpha_i \geq 0 \forall i$ . Therefore, the LPV system representation is given as a convex combination of the state-space realizations of the LTI systems given at the vertices  $w_i$ :

$$\left[ \begin{array}{c|cc} A(\rho) & B_1(\rho) & B_2 \\ \hline C_1(\rho) & D_{11}(\rho) & D_{12} \\ C_2 & D_{21} & 0 \end{array} \right] = \sum_{i=1}^{2^{n_p}} \alpha_i(\rho) \left[ \begin{array}{c|cc} A_i & B_{1,i} & B_2 \\ \hline C_{1,i} & D_{11,i} & D_{12} \\ C_2 & D_{21} & 0 \end{array} \right] \quad (10)$$

Now, assume that

**Assumption 1.** There exists an LPV output-feedback controller  $K^{(0)}(\rho)$  which quadratically stabilizes  $G(\rho)$  over  $\mathcal{P}$  (following the approach in<sup>8</sup>), defined as:

$$K^{(0)}(\rho) : \left[ \begin{array}{c|c} A_k^{(0)}(\rho) & B_k^{(0)}(\rho) \\ \hline C_k^{(0)}(\rho) & D_k^{(0)}(\rho) \end{array} \right] \quad (11)$$

being,

$$\left[ \begin{array}{c|c} A_k^{(0)}(\rho) & B_k^{(0)}(\rho) \\ \hline C_k^{(0)}(\rho) & D_k^{(0)}(\rho) \end{array} \right] = \sum_{i=1}^{2^{n_p}} \alpha_i(\rho) \left[ \begin{array}{c|c} A_{k,i}^{(0)} & B_{k,i}^{(0)} \\ \hline C_{k,i}^{(0)} & D_{k,i}^{(0)} \end{array} \right] \quad (12)$$

where  $A_k^{(0)}(\rho) \in \mathbb{R}^{n_k^{(0)} \times n_k^{(0)}}$ ,  $B_k^{(0)}(\rho) \in \mathbb{R}^{n_k^{(0)} \times m_k}$ ,  $C_k^{(0)}(\rho) \in \mathbb{R}^{p_k \times n_k^{(0)}}$  and  $D_k^{(0)}(\rho) \in \mathbb{R}^{p_k \times m_k}$ .

**Assumption 2.** At each vertex  $w_i$  ( $i \in \llbracket 1, 2^{n_p} \rrbracket$ ) of the polytope  $\mathcal{P}$ , a group of  $\zeta$  local LTI controllers  $K_i^{(j)}$  ( $j \in \llbracket 1, \zeta \rrbracket$ ) have been designed independently to stabilize  $G_i$  achieving different objectives and performances for all operating conditions.

### 3.2 Problem Definition

The main argument behind this study is that, in real application cases, it may be difficult to find a single LPV controller covering multiple closed-loop performances over the whole parameter region. Therefore the objective of this work is mainly to:

1. Design a set of gain-scheduled controllers  $K^{(j)}(\rho)$ ,  $j \in \llbracket 1, \zeta \rrbracket$ . Each one is designed by interpolating its corresponding LTI controllers  $K_i^{(j)}$  ( $i \in \llbracket 1, 2^{n_p} \rrbracket$ ) based on the proposed approach in<sup>21</sup>.

2. Create an overall interpolation scheme between the gain-scheduled controllers  $K^{(j)}(\rho)$  ( $j \in \llbracket 0, \zeta \rrbracket$ ), by an interpolating signal vector  $\gamma$ , which is referred to  $\tilde{K}(\rho, \gamma)$ , such that the resultant LPV-YK controller  $\tilde{K}(\rho, \gamma)$  quadratically stabilizes  $G(\rho) \forall \rho \in \mathcal{P}$  and for every  $\gamma = [\gamma_1, \dots, \gamma_j, \dots, \gamma_\zeta]$ .

Figure 1 represents an example of an LPV-YK based interpolation between three gain scheduled-scheduled controllers  $K^{(0)}(\rho)$ ,  $K^{(1)}(\rho)$ , and  $K^{(2)}(\rho)$ , along the convex parameter space  $\mathcal{P}$ . The orange solid line represents the chosen nominal LPV controller  $K^{(0)}(\rho)$ , as defined by **Assumption 1**. The blue/red points represent the local LTI controllers  $K_i^{(1)}/K_i^{(2)}$  ( $i \in \llbracket 1, 2^{n_p} \rrbracket$ ) as defined in **Assumption 2**. The blue/red dashed line is the gain-scheduled controller  $K^{(1)}(\rho)/K^{(2)}(\rho)$  that is designed by the YK-based interpolation of the LTI controllers  $K_i^{(j)}/K_i^{(2)}$ . The overall interpolation is performed using the interpolating signal  $\gamma = [\gamma_1, \gamma_2]$ , and is represented by the LPV-YK controller  $\tilde{K}(\rho, \gamma)$ .

## 4 Main Result

Based on the statements on LPV concepts and YK parameterization, an LPV-YK controller  $\tilde{K}(\rho, \gamma)$  is designed to achieve a quadratically stable interpolation between multiple LPV controllers  $K^{(j)}(\rho)$  ( $j \in \llbracket 0, \zeta \rrbracket$ ). Its state-space realization is defined as:

$$\tilde{K}(\rho, \gamma) : \left[ \begin{array}{c|c} \tilde{A}_k(\rho, \gamma) & \tilde{B}_k(\rho, \gamma) \\ \hline \tilde{C}_k(\rho, \gamma) & \tilde{D}_k(\rho, \gamma) \end{array} \right] \quad (13)$$

Each LPV controller  $K^{(j)}(\rho)$  ( $j \in \llbracket 1, \zeta \rrbracket$ ) is designed based on Linear Matrix Inequality (LMI) optimization problem as proposed by<sup>21</sup>. The difference is that here we parameterize the LTI controllers, at the polytopic vertices, with respect to a dynamic LPV controller  $K^{(0)}(\rho)$  instead of a state-feedback as represented in<sup>21</sup>.

An interpolating signal vector  $\gamma$  is included to interpolate between the LPV controllers. The interest of the YK parameterization is that, depending on  $\gamma$ , several interpolation cases can be obtained, in particular allowing for  $\tilde{K}(\rho, \gamma)$  to recover a single gain-scheduled controller  $K^{(j)}(\rho)$  by varying  $\gamma_j$ :

- if  $\gamma_j = 0 \forall j$ ,  $\tilde{K}(\rho, \gamma) \equiv K^{(0)}(\rho) = \sum_{i=1}^{2^{n_p}} \alpha_i(\rho) K_i^{(0)}$
- if  $\gamma_j = 1$  for  $j = c \in [1, \zeta]$  and  $\gamma_j = 0 \forall j \neq c$ ,  $\tilde{K}(\rho, \gamma) \equiv K^{(c)}(\rho) = \sum_{i=1}^{2^{n_p}} \alpha_i(\rho) K_i^{(c)}$
- else, the performance of  $\tilde{K}(\rho, \gamma)$  is interpolated among  $K^{(j)}(\rho)$  according to the chosen  $\gamma_j$ .

The following theorem aims to prove that  $\tilde{K}(\rho, \gamma)$  quadratically stabilizes  $G(\rho)$  for every  $\rho \in \mathcal{P}$  and for every continuous/discontinuous interpolating signals  $\gamma$ .

**Theorem 1.** Consider an LPV plant  $G(\rho)$  (7), satisfying assumptions **Assumption 1** and **Assumption 2**. Then, the following generalized LPV-YK controller  $\tilde{K}(\rho, \gamma)$  (17) quadratically stabilizes  $G(\rho)$  for any  $\rho \in \mathcal{P}$  and for any continuous/discontinuous interpolating signals  $\gamma_j \in [0, 1]$  ( $j \geq 1$ ), if there exist symmetric, positive definite, constant matrices  $X_g \in \mathbb{R}^{n_x \times n_x}$ ,  $X_{q,i}^{(j)} = \text{diag}(S_i^{(j)}, R_i) \in \mathbb{R}^{n_{q,i}^{(j)} \times n_{q,i}^{(j)}}$ , and  $X_{k,i} \in \mathbb{R}^{n_k^{(0)} \times n_k^{(0)}}$ , and matrices  $W_i$  and  $V_i$  such that  $\forall i$ :

$$A_i X_g + X_g A_i^T + B_2 W_i + W_i^T B_2^T < 0 \quad \forall w_i \quad (14)$$

$$A_{k,i}^{(0)} X_{k,i} + X_{k,i} A_{k,i}^{(0)T} + B_{k,i}^{(0)} V_i + V_i^T B_{k,i}^{(0)T} < 0 \quad \forall w_i \quad (15)$$

$$X_{q,i}^{(j)} A_{q,i}^{(j)} + (A_{q,i}^{(j)})^T X_{q,i}^{(j)} < 0 \quad \forall w_i, \forall j \quad (16)$$

$$\text{with } A_{q,i}^{(j)} = \left[ \begin{array}{ccc} A_i + B_2 D_{k,i}^{(j)} C_2 & B_2 C_{k,i}^{(j)} & B_2 [D_{k,i}^{(j)} - D_{k,i}^{(0)}] F_{k,i}^{(0)} - B_2 C_{k,i}^{(0)} \\ B_{k,i}^{(j)} C_2 & A_{k,i}^{(j)} & B_{k,i}^{(j)} F_{k,i}^{(0)} \\ 0 & 0 & A_{k,i}^{(0)} + B_{k,i}^{(0)} F_{k,i}^{(0)} \end{array} \right], \text{ and } F_{k,i}^{(0)} = V_i X_{k,i}^{-1}.$$



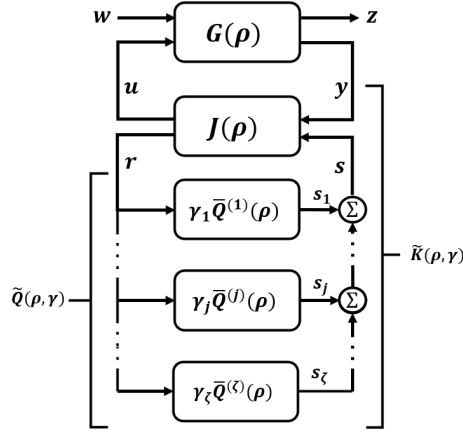


FIGURE 2 LPV-YK closed-loop LFT configuration

The state-space matrices of  $\tilde{K}(\rho, \gamma)$  are

$$\begin{aligned} \tilde{A}_k(\rho, \gamma) &= \sum_{i=1}^{2^{n_p}} \alpha_i(\rho) \begin{bmatrix} A_i + B_2 F_{g,i} - B_2 \tilde{D}_{q,i}(\gamma) C_2 & -B_2 \tilde{D}_{q,i}(\gamma) F_{k,i}^{(0)} & B_2 \tilde{C}_{q,i}(\gamma) \\ -B_{k,i}^{(0)} C_2 & A_{k,i}^{(0)} & 0 \\ -\tilde{B}_{q,i} C_2 & -\tilde{B}_{q,i} F_{k,i}^{(0)} & \tilde{A}_{q,i} \end{bmatrix} \\ \tilde{B}_k(\rho, \gamma) &= \sum_{i=1}^{2^{n_p}} \alpha_i(\rho) \begin{bmatrix} B_2 \tilde{D}_{q,i}(\gamma) \\ B_{k,i}^{(0)} \\ \tilde{B}_{q,i} \end{bmatrix} \\ \tilde{C}_k(\rho, \gamma) &= \sum_{i=1}^{2^{n_p}} \alpha_i(\rho) \begin{bmatrix} F_{g,i} - (D_{k,i}^{(0)} + \tilde{D}_{q,i}(\gamma)) C_2 & C_{k,i}^{(0)} - \tilde{D}_{q,i}(\gamma) F_{k,i}^{(0)} & \tilde{C}_{q,i}(\gamma) \end{bmatrix} \\ \tilde{D}_k(\rho, \gamma) &= \sum_{i=1}^{2^{n_p}} \alpha_i(\rho) [D_{k,i}^{(0)} + \tilde{D}_{q,i}(\gamma)] \end{aligned} \quad (17)$$

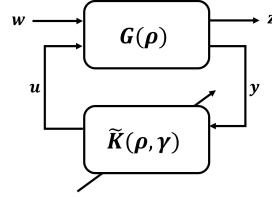
where  $\forall i \in \llbracket 1, 2^{n_p} \rrbracket$ ,  $F_{g,i} = W_i X_g^{-1}$  and

$$\begin{aligned} \tilde{A}_{q,i} &= \text{diag}(Z_i^{(1)} A_{q,i}^{(1)} (Z_i^{(1)})^{-1}, \dots, Z_i^{(j)} A_{q,i}^{(j)} (Z_i^{(j)})^{-1}, \dots, Z_i^{(\zeta)} A_{q,i}^{(\zeta)} (Z_i^{(\zeta)})^{-1}), \\ \tilde{B}_{q,i} &= \begin{bmatrix} Z_i^{(1)} B_{q,i}^{(1)} & \dots & Z_i^{(j)} B_{q,i}^{(j)} & \dots & Z_i^{(\zeta)} B_{q,i}^{(\zeta)} \end{bmatrix}^T, \\ \tilde{C}_{q,i}(\gamma) &= \begin{bmatrix} \gamma_1 C_{q,i}^{(1)} (Z_i^{(1)})^{-1} & \dots & \gamma_j C_{q,i}^{(j)} (Z_i^{(j)})^{-1} & \dots & \gamma_\zeta C_{q,i}^{(\zeta)} (Z_i^{(\zeta)})^{-1} \end{bmatrix}, \\ \tilde{D}_{q,i}(\gamma) &= \sum_{j=1}^{\zeta} \gamma_j D_{q,i}^{(j)}, \end{aligned} \quad (18)$$

where  $Z_i^{(j)} = (X_{q,i}^{(j)})^{1/2}$ .

**Proof 1.** According to YK parameterization concept, each parameterized controller can be formulated as a Linear Fractional Transformation (LFT) system, refer to chapter 2 in<sup>29</sup>. Then, the LPV-YK controller can be written as  $\tilde{K}(\rho, \gamma) = F_l(J(\rho), \tilde{Q}(\rho, \gamma))$  (see Fig. 2), where  $J(\rho)$  is represented in (19), and  $\tilde{Q}(\rho, \gamma) = \sum_{j=1}^{\zeta} \gamma_j(t) \tilde{Q}^{(j)}(\rho) = \sum_{j=1}^{\zeta} \gamma_j \sum_{i=1}^{2^{n_p}} \alpha_i \tilde{Q}_i^{(j)}$  being  $\tilde{Q}_i^{(j)}$  a transformed system of  $Q_i^{(j)}$  (20) by the transformation matrix  $Z_i^{(j)}$ .

$$Q^{(j)}(\rho) = \sum_{i=1}^{2^{n_p}} \alpha_i(\rho) \left[ \begin{array}{c|c} A_{q,i}^{(j)} & B_{q,i}^{(j)} \\ \hline C_{q,i}^{(j)} & D_{q,i}^{(j)} \end{array} \right] = \sum_{i=1}^{2^{n_p}} \alpha_i(\rho) \left[ \begin{array}{ccc|c} A_i + B_2 D_{k,i}^{(j)} C_2 & B_2 C_{k,i}^{(j)} & B_2 [D_{k,i}^{(j)} - D_{k,i}^{(0)}] F_{k,i}^{(0)} - B_2 C_{k,i}^{(0)} & B_2 [D_{k,i}^{(j)} - D_{k,i}^{(0)}] \\ B_{k,i}^{(j)} C_2 & A_{k,i}^{(j)} & B_{k,i}^{(j)} F_{k,i}^{(0)} & B_{k,i}^{(j)} \\ \hline 0 & 0 & A_{k,i}^{(0)} + B_{k,i}^{(0)} F_{k,i}^{(0)} & B_{k,i}^{(0)} \\ \hline [D_{k,i}^{(j)} C_2 - F_{g,i}] & C_{k,i}^{(j)} & [(D_{k,i}^{(j)} - D_{k,i}^{(0)}) F_{k,i}^{(0)} - C_{k,i}^{(0)}] & [D_{k,i}^{(j)} - D_{k,i}^{(0)}] \end{array} \right] \quad (20)$$

FIGURE 3  $G - \tilde{K}$  LFT interconnection

$$J(\rho) = \sum_{i=1}^{2^{n_p}} \alpha_i(\rho) \left[ \begin{array}{cc|cc} A_i + B_2 F_{g,i} & 0 & 0 & B_2 \\ -B_{k,i}^{(0)} C_2 & A_{k,i}^{(0)} & B_{k,i}^{(0)} & 0 \\ \hline F_{g,i} - D_{k,i}^{(0)} C_2 & C_{k,i}^{(0)} & D_{k,i}^{(0)} & I \\ -C_2 & -F_{k,i}^{(0)} & I & 0 \end{array} \right] \quad (19)$$

The closed-loop system  $CL(\rho, \gamma) = \mathcal{F}_l(G(\rho), \tilde{K}(\rho, \gamma))$  (21) is derived from the LFT interconnection between  $G(\rho)$  and  $\tilde{K}(\rho, \gamma)$  from the input  $w$  to the output  $z$  (see Fig. 3), as:

$$CL(\rho, \gamma) = \sum_{i=1}^{2^{n_p}} \alpha_i(\rho) \left[ \begin{array}{ccc|c} A_i + B_2 (D_{k,i}^{(0)} + \tilde{D}_{q,i}(\gamma)) C_2 & B_2 (F_{g,i} - (D_{k,i}^{(0)} + \tilde{D}_{q,i}(\gamma)) C_2) & B_2 (C_{k,i}^{(0)} - \tilde{D}_{q,i}(\gamma) F_{k,i}^{(0)}) & \\ B_2 \tilde{D}_{q,i}(\gamma) C_2 & A_i + B_2 (F_{g,i} - \tilde{D}_{q,i}(\gamma) C_2) & -B_2 \tilde{D}_{q,i}(\gamma) F_{k,i}^{(0)} & \\ B_{k,i}^{(0)} C_2 & -B_{k,i}^{(0)} C_2 & A_{k,i}^{(0)} & \\ \tilde{B}_{q,i} C_2 & -\tilde{B}_{q,i} C_2 & -\tilde{B}_{q,i} F_{k,i}^{(0)} & \\ \hline C_{1,i} + D_{12} (D_{k,i}^{(0)} + \tilde{D}_{q,i}(\gamma)) C_2 & D_{12} (F_{g,i} - (D_{k,i}^{(0)} + \tilde{D}_{q,i}(\gamma)) C_2) & D_{12} (C_{k,i}^{(0)} - \tilde{D}_{q,i}(\gamma) F_{k,i}^{(0)}) & \\ \hline B_2 \tilde{C}_{q,i}(\gamma) & B_{1,i} + B_2 (D_{k,i}^{(0)} + \tilde{D}_{q,i}(\gamma)) D_{21} & & \\ B_2 \tilde{C}_{q,i}(\gamma) & B_2 \tilde{D}_{q,i}(\gamma) D_{21} & & \\ 0 & B_{k,i}^{(0)} D_{21} & & \\ \tilde{A}_{q,i} & \tilde{B}_{q,i} D_{21} & & \\ \hline D_{12} \tilde{C}_{q,i}(\gamma) & D_{11,i} + D_{12} (D_{k,i}^{(0)} + \tilde{D}_{q,i}(\gamma)) D_{21} & & \end{array} \right]$$

$$= \sum_{i=1}^{2^{n_p}} \alpha_i(\rho) \left[ \begin{array}{c|c} A_{cl}(\rho, \gamma) & B_{cl}(\rho, \gamma) \\ \hline C_{cl}(\rho, \gamma) & D_{cl}(\rho, \gamma) \end{array} \right] \quad (21)$$

The closed-loop state matrix above  $A_{cl}(\rho, \gamma) = \sum_{i=1}^{2^{n_p}} \alpha_i(\rho) A_{cl,i}(\gamma)$  is quadratically stable if there exist a symmetric, positive definite, constant matrix  $X_{cl}$  such that:

$$X_{cl} A_{cl}(\rho, \gamma) + A_{cl}^T(\rho, \gamma) X_{cl} < 0 \quad \forall \rho, \forall \gamma \quad (22)$$

Now, let  $T = \begin{bmatrix} I & 0 & 0 & 0 \\ 0 & 0 & 0 & I \\ I & -I & 0 & 0 \\ 0 & 0 & I & 0 \end{bmatrix}$  be a state transformation matrix which is applied to  $CL(\rho, \gamma)$  without changing its input-output nature, with  $T^{-1} = \begin{bmatrix} I & 0 & 0 & 0 \\ I & 0 & -I & 0 \\ 0 & 0 & 0 & I \\ 0 & I & 0 & 0 \end{bmatrix}$ . Then it comes,

$$\bar{A}_{cl}(\rho, \gamma) = \sum_{i=1}^{2^{np}} \alpha_i(\rho) T A_{cl,i}(\gamma) T^{-1} = \sum_{i=1}^{2^{np}} \alpha_i(\rho) \begin{bmatrix} A_i + B_2 F_{g,i} & B_2 \tilde{C}_{q,i}(\gamma) & -B_2(F_{g,i} - (D_{k,i}^{(0)} + \tilde{D}_{q,i}(\gamma))C_2) & B_2(C_{k,i}^{(0)} - \tilde{D}_{q,i}(\gamma)F_{k,i}^{(0)}) \\ 0 & \tilde{A}_{q,i} & \tilde{B}_{q,i}C_2 & -\tilde{B}_{q,i}F_{k,i}^{(0)} \\ 0 & 0 & A_i + B_2 D_{k,i}^{(0)}C_2 & B_2 C_{k,i}^{(0)} \\ 0 & 0 & B_{k,i}^{(0)}C_2 & A_{k,i}^{(0)} \end{bmatrix} \quad (23)$$

Due to the block-triangular form of  $\bar{A}_{cl}(\rho, \gamma)$  (23), (22) is satisfied if the following equations hold (check Lemma 2 in<sup>25</sup>):

$$\sum_{i=1}^{2^{np}} \alpha_i(\rho) (Y_g (A_i + B_2 F_{g,i}) + (A_i + B_2 F_{g,i})^T Y_g) < 0 \quad (24)$$

$$\sum_{i=1}^{2^{np}} \alpha_i(\rho) (Y_q \tilde{A}_{q,i} + \tilde{A}_{q,i}^T Y_q) < 0 \quad (25)$$

$$\sum_{i=1}^{2^{np}} \alpha_i(\rho) (Y_0 A_i^{(0)} + A_i^{(0)T} Y_0) < 0 \quad (26)$$

where  $Y_g \in \mathbb{R}^{n_x \times n_x}$ ,  $Y_q \in \mathbb{R}^{n_q^{(1)} \times n_q^{(1)}}$  and  $Y_0 \in \mathbb{R}^{(n_x + n_k^{(0)}) \times (n_x + n_k^{(0)})}$  are symmetric, positive definite, parameter-invariant matrices, with  $X_{cl} = T^T \text{diag}(Y_g, Y_q, Y_0) T$ , and

$$A_i^{(0)} = \begin{bmatrix} A_i + B_2 D_{k,i}^{(0)}C_2 & B_2 C_{k,i}^{(0)} \\ B_{k,i}^{(0)}C_2 & A_{k,i}^{(0)} \end{bmatrix} \quad (27)$$

In order to verify the inequalities (24)-(26), a two-steps procedure is detailed:

1. Prove that (24) and (26) are satisfied
2. Prove that the state matrix  $\tilde{A}_q(\rho)$  is quadratically stable  $\forall \rho \in \mathcal{P}$ .

### Step 1:

Inequality (24) is equivalent to (14) by choosing  $Y_g = X_g^{-1}$  and  $W_i = F_{g,i} X_g$ . (26) is fulfilled given that  $K^{(0)}(\rho)$  quadratically stabilizes  $G(\rho)$ .

### Step 2:

Recall that  $\tilde{A}_{q,i} = \text{diag}(Z_i^{(1)} A_{q,i}^{(1)} (Z_i^{(1)})^{-1}, \dots, Z_i^{(j)} A_{q,i}^{(j)} (Z_i^{(j)})^{-1}, \dots, Z_i^{(\xi)} A_{q,i}^{(\xi)} (Z_i^{(\xi)})^{-1})$ .

Thus, inequality (25) is satisfied if it is proved that each transformed  $\bar{A}_q^{(j)}(\rho) = \sum_{i=1}^{2^{np}} \alpha_i(\rho) Z_i^{(j)} A_{q,i}^{(j)} (Z_i^{(j)})^{-1}$  is quadratically stable ( $\forall j \geq 1$ ). Let us prove that there exist symmetric, positive definite matrices  $Y_q^{(j)} \in \mathbb{R}^{n_q^{(j)} \times n_q^{(j)}}$  such that:

$$\sum_{i=1}^{2^{np}} \alpha_i(\rho) (Y_q^{(j)} \bar{A}_{q,i}^{(j)} + \bar{A}_{q,i}^{(j)T} Y_q^{(j)}) < 0 \quad \forall j \quad (28)$$

Regarding eq. (20), notice that  $A_{q,i}^{(j)}$  is Hurwitz by design since it is triangular with two stable diagonal elements. The upper diagonal element is stable since  $K_i^{(j)}$  stabilizes  $G_i^{(j)} \forall i, j$  (from **Assumption 2**). The second diagonal element is stable by choosing  $V_i = F_{k,i}^{(0)} X_{k,i}$  in inequality (15).

For each  $j \geq 1$ , since  $A_{q,i}^{(j)}$  are Hurwitz matrices, and according to **Lemma 1**, if  $X_{q,i}^{(j)} = Z_i^{(j)T} Y_q^{(j)} Z_i^{(j)}$ , inequality (16) is

equivalent to (28). Thus, (28) is verified and  $\tilde{A}_q^{(j)}(\rho)$  is quadratically stable  $\forall j$ , and consequently, (25) is satisfied with  $Y_q = \text{diag}(Y_q^{(1)} \dots Y_q^{(\zeta)})$ .

As a result, the inequality (22) holds and thus  $CL(\rho, \gamma)$  is quadratically stable  $\forall \rho \forall \gamma$ .

**Remark 1.** It is worth mentioning that the problem complexity refers mainly to find a nominal LPV controller  $K^{(0)}(\rho)$  which must quadratically stabilize  $G(\rho)$ , i.e. assumption **Assumption 1**. The rest is carried out using classical LTI control approaches. This shows an interest since a quadratically stabilizing gain-scheduled controller  $K^{(j)}(\rho)$  could be designed based on an interpolation of LTI controllers, with lower conservatism compared to the standard polytopic design<sup>8</sup>. In addition, the interpolation of these gain-scheduled controllers, with any finite continuous/discontinuous interpolating signals  $\gamma_j$ , provides a general multi-variable and multi-objective controller  $\tilde{K}(\rho, \gamma)$  based on LPV-YK concept.

## 5 LPV-YK Control Implementation

In this section, the implementation scheme of the LPV-YK control is formulated using the doubly coprime factorization<sup>40</sup>.

### 5.1 Coprime Factorization

Using the doubly coprime factorization concept, at each vertex  $w_i$  of  $\mathcal{P}$ , the plant model  $G_i$  and the controllers  $K_i^{(j)}$ ,  $\forall i \in \llbracket 1, 2^{n_p} \rrbracket$  and  $\forall j \in \llbracket 0, \zeta \rrbracket$ , can be factorised as:

$$\begin{aligned} G_i &= N_i M_i^{-1} = \tilde{M}_i^{-1} \tilde{N}_i \\ K_i^{(j)} &= U_i^{(j)} V_i^{(j)-1} = \tilde{V}_i^{(j)-1} \tilde{U}_i^{(j)} \end{aligned} \quad (29)$$

**Lemma 2** is applied  $\forall i, \forall j$ , where the coprime factors are computed such that  $M_i, N_i, \tilde{M}_i, \tilde{N}_i, U_i^{(j)}, V_i^{(j)}, \tilde{U}_i^{(j)}, \tilde{V}_i^{(j)} \in \mathcal{RH}_\infty$  and satisfying the following *Bezout Identity*:

$$\begin{bmatrix} \tilde{V}_i^{(j)} & -\tilde{U}_i^{(j)} \\ -\tilde{N}_i & \tilde{M}_i \end{bmatrix} \begin{bmatrix} M_i & U_i^{(j)} \\ N_i & V_i^{(j)} \end{bmatrix} = \begin{bmatrix} M_i & U_i^{(j)} \\ N_i & V_i^{(j)} \end{bmatrix} \begin{bmatrix} \tilde{V}_i^{(j)} & -\tilde{U}_i^{(j)} \\ -\tilde{N}_i & \tilde{M}_i \end{bmatrix} = \begin{bmatrix} I & 0 \\ 0 & I \end{bmatrix} \quad (30)$$

The coprime factors are computed at each vertex using the state-space representations written in (31)-(32).

$$\begin{bmatrix} M_i & U_i^{(j)} \\ N_i & V_i^{(j)} \end{bmatrix} : \left[ \begin{array}{cc|cc} A_i + B_2 F_{g,i} & 0 & B_2 & 0 \\ 0 & A_{k,i}^{(j)} + B_{k,i}^{(j)} F_{k,i}^{(j)} & 0 & B_{k,i}^{(j)} \\ F_{g,i} & C_{k,i}^{(j)} + D_{k,i}^{(j)} F_{k,i}^{(j)} & I & D_{k,i}^{(j)} \\ C_2 & F_{k,i}^{(j)} & 0 & I \end{array} \right] \quad (31)$$

$$\begin{bmatrix} \tilde{V}_i^{(j)} & -\tilde{U}_i^{(j)} \\ -\tilde{N}_i & \tilde{M}_i \end{bmatrix} : \left[ \begin{array}{cc|cc} A_i + B_2 D_{k,i}^{(j)} C_2 & B_2 C_{k,i}^{(j)} & -B_2 & B_2 D_{k,i}^{(j)} \\ B_{k,i}^{(j)} C_2 & A_{k,i}^{(j)} & 0 & B_{k,i}^{(j)} \\ F_{g,i} - D_{k,i}^{(j)} C_2 & -C_{k,i}^{(j)} & I & -D_{k,i}^{(j)} \\ C_2 & -F_{k,i}^{(j)} & 0 & I \end{array} \right] \quad (32)$$

### 5.2 LPV-YK Control Structure

Recall that  $K^{(0)}(\rho)$  is previously designed to quadratically stabilize  $G(\rho)$  (7), and the gain-scheduled controllers  $K^{(j)}(\rho)$  are designed using **Theorem 1** to quadratically stabilize  $G(\rho)$ . Following **Lemma 3**, and choosing  $K^{(0)}(\rho)$  as the nominal controller, the generalized LPV-YK controller  $\tilde{K}(\rho, \gamma)$  can be expressed as:

$$\begin{aligned} \tilde{K}(\rho, \gamma) &= \left( U^{(0)}(\rho) + M(\rho) \sum_{j=1}^{\zeta} \gamma_j \bar{Q}^{(j)}(\rho) \right) \left( V^{(0)}(\rho) + N(\rho) \sum_{j=1}^{\zeta} \gamma_j \bar{Q}^{(j)}(\rho) \right)^{-1} \\ &= \left( \tilde{V}^{(0)}(\rho) + \sum_{j=1}^{\zeta} \gamma_j \bar{Q}^{(j)}(\rho) \tilde{N}(\rho) \right)^{-1} \left( \tilde{U}^{(0)}(\rho) + \sum_{j=1}^{\zeta} \gamma_j \bar{Q}^{(j)}(\rho) \tilde{M}(\rho) \right) \end{aligned} \quad (33)$$

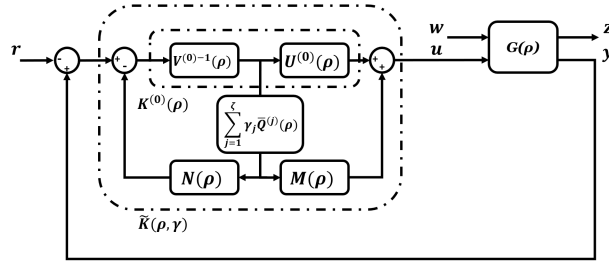


FIGURE 4 YK control structure

### 5.3 How to choose the interpolating signal vector $\gamma$

$\gamma$  is a vector of interpolating signals  $\gamma_j$ , where each one multiplies its corresponding output of  $\bar{Q}^{(j)}(\rho)$  to interpolate between several parameterized controllers  $K^{(j)}(\rho) = \mathcal{F}_l(J(\rho), \bar{Q}^{(j)}(\rho))$ . Notice that  $\gamma_j$  could be any ad-hoc physically based, continuous/discontinuous, external or internal signals. Theoretically, and according to the proof above, the closed-loop quadratic stability is achieved for any  $\gamma_j$  having finite positive/negative value with any rate of variation. However, for control interpolation, the interpolating signals  $\gamma_j$  are chosen to be in  $[0, 1]$ . In this paper,  $\gamma_j$  are chosen as

$$\sum_{j=1}^{\zeta} \gamma_j = 1, \quad \gamma_j \in [0, 1] \quad \forall j \quad (34)$$

### 5.4 Local LTI Control Performance Recovery

In this section, the performance recovery of each pre-designed local LTI controller  $K_i^{(j)}$  ( $i \in [1, 2^{n_p}]$ ,  $j \geq 1$ ), from the LPV-YK controller  $\tilde{K}(\rho, \gamma)$ , is verified. Let us choose an LTI controller  $K_i^{(c)}$  (i.e.  $\gamma_c = 1$  and  $\gamma_j = 0 \quad \forall j \neq c$ , and  $\rho = w_l$ ). The following derivation shows the performance recovery of  $K_i^{(c)}$  from  $\tilde{K}(\rho, \gamma)$ :

Substitute the vertex  $w_l^{(c)}$  and  $\gamma = [0 \dots 0 \quad \gamma_c = 1 \quad 0 \dots 0]$  (denoted by  $\gamma_c^* = 1$ ) in (33),

$$\tilde{K}(w_l, \gamma_c^* = 1) = \left( U_l^{(0)} + M_l \bar{Q}_l^{(c)} \right) \left( V_l^{(0)} + N_l \bar{Q}_l^{(c)}(\rho) \right)^{-1} \quad (35)$$

Since the input-output performance of  $Q$  and  $\bar{Q}$  is similar (according to the state transformation concept),  $\bar{Q}_l^{(0)} \equiv Q_l^{(0)}$ . According to<sup>29</sup>, (35) can be written as

$$\tilde{K}(w_l, \gamma_c^* = 1) = U_l^{(0)} (V_l^{(0)})^{-1} + (\tilde{V}_l^{(0)})^{-1} Q_l^{(c)} \left( I + (V_l^{(0)})^{-1} N_l^{(0)} Q_l^{(c)} \right)^{-1} (V_l^{(0)})^{-1} \quad (36)$$

Referring to YK concept,  $Q_l^{(c)} = \tilde{V}_l^{(c)} V_l^{(0)} - \tilde{V}_l^{(c)} U_l^{(0)}$ , after some derivations:

$$\begin{aligned} Q_l^{(c)} &= \tilde{V}_l^{(c)} (\tilde{V}_l^{(c)})^{-1} \tilde{V}_l^{(c)} V_l^{(0)} - \tilde{V}_l^{(c)} U_l^{(0)} (V_l^{(0)})^{-1} V_l^{(0)} \\ &= \tilde{V}_l^{(c)} K_l^{(c)} V_l^{(0)} - \tilde{V}_l^{(c)} K_l^{(0)} V_l^{(0)} \\ &= \tilde{V}_l^{(c)} (K_l^{(c)} - K_l^{(0)}) V_l^{(0)} \end{aligned} \quad (37)$$

Substitute and shape it, then

$$\tilde{K}(w_l, \gamma_c^* = 1) = K_l^{(0)} + [\tilde{V}_l^{(c)} V_l^{(0)} + (K_l^{(c)} - K_l^{(0)}) N_l \tilde{V}_l^{(0)}]^{-1} \times (K_l^{(c)} - K_l^{(0)}) \quad (38)$$

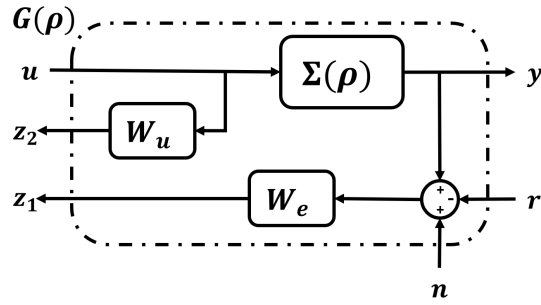
Knowing that  $K_l^{(c)} = (\tilde{V}_l^{(c)})^{-1} \tilde{U}_l^{(c)}$ , and applying the Bezout identities (30), we get:

$$\tilde{V}_l^{(c)} V_l^{(0)} + (K_l^{(c)} - K_l^{(0)}) N_l \tilde{V}_l^{(0)} = I. \quad (39)$$

Then,

$$\tilde{K}(w_l, \gamma_c^* = 1) = K_l^{(0)} + K_l^{(c)} - K_l^{(0)} = K_l^{(c)}. \quad (40)$$

Therefore, it is shown that the performance achieved by the LPV-YK controller  $\tilde{K}(\rho, \gamma)$  at any vertex  $w_l$  is equivalent to the performance of its corresponding LTI controller  $K_l^{(c)}$ .

FIGURE 5 Generalized Plant  $G(\rho)$ 

## 6 Application to Autonomous Vehicles

The proposed method is applied here to the autonomous vehicle lateral control.<sup>39</sup> compares three LPV control approaches where the longitudinal speed is considered as the varying parameter. In addition, lateral control aims to achieve various objectives such as lane tracking, lane changing, obstacle avoidance, etc. Consequently, various performances are required accordingly for different traffic situations that faces the vehicle. Thus, an LPV-YK controller could be designed to achieve multiple objectives, depending on the driving situation, over the full vehicle speed range.

### 6.1 Lateral Bicycle Model

We consider here the well known bicycle model of an autonomous vehicle. The non-linear lateral dynamics can be written as a polytopic LPV model  $\Sigma(\rho)$ <sup>39</sup>:

$$\Sigma(\rho) \begin{cases} \dot{x}(t) = A_{\Sigma}(\rho)x(t) + B_{\Sigma}u(t) \\ y(t) = C_{\Sigma}x(t) \end{cases} \quad (41)$$

being

$$x(t) = \begin{bmatrix} v_y \\ w \end{bmatrix}, \quad u(t) = \delta, \quad B_{\Sigma} = \begin{bmatrix} \frac{1}{I} C_f \\ \frac{1}{I} C_f l_f \end{bmatrix}, \quad C_{\Sigma} = [0 \ 1], \quad A_{\Sigma}(\rho) = \begin{bmatrix} -\frac{C_r + C_f}{m} \rho_2 & -\frac{C_f l_f - C_r l_r}{I} \rho_2 - \rho_1 \\ -\frac{C_f l_f - l_r C_r}{I} \rho_2 & -\frac{C_f l_f^2 + l_r^2 C_r}{I} \rho_2 \end{bmatrix}, \quad (42)$$

where  $\rho = [\rho_1, \rho_2] = [v_x, \frac{1}{v_x}]$ .  $v_x$  represents the longitudinal speed which varies in  $[1, 30]$  m/s.  $v_y$  and  $w$  are the lateral and rotational velocities in the vehicle's frame, respectively.  $\delta$  is the control input, the steering angle of the front tire.  $C_f$  and  $C_r$  represent the stiffness of the front and rear wheel-tires.  $I$ ,  $m$ ,  $l_f$  and  $l_r$  are the vehicle's inertia, mass and the distance from the center of gravity to the front and rear wheel axes respectively.

### 6.2 Lateral Control Design

In this work, the control design problems (mentioned in **Assumption 1- Assumption 2**) are solved using the  $\mathcal{H}_{\infty}$  concept. For control design purpose, two weighting transfer functions  $W_e(s)$  and  $W_u(s)$  are designed to present the tracking performance and the actuator limitations respectively. Then, the state-space representation of  $G(\rho)$  is obtained from the generalized plant shown in Fig. 5.  $G(\rho)$  is written as a convex combination of the vertices of the polytope  $\mathcal{P} = C_{\mathcal{O}}\{(\underline{\rho}_1, \underline{\rho}_2), (\underline{\rho}_1, \overline{\rho}_2), (\overline{\rho}_1, \underline{\rho}_2), (\overline{\rho}_1, \overline{\rho}_2)\}$  (refer to (9)-(10)).

Now, following **Assumption 1- Assumption 2**, a highly robust LPV controller  $K^{(0)}(\rho)$ , and two gain-scheduled controllers  $K^{(1)}(\rho)$  and  $K^{(2)}(\rho)$  are designed to perform different required performances as follows:

- The polytopic-based LPV controller  $K^{(0)}(\rho)$  is designed using the  $\mathcal{H}_{\infty}$  concept following a method similar to<sup>8</sup>. A slow transient response and noise rejection performances are required for the nominal controller  $K^{(0)}(\rho)$  using weighting functions  $W_e^{(0)}$  and  $W_u^{(0)}$ .
- LTI controllers  $K_i^{(1)}$  are designed separately using LTI/ $\mathcal{H}_{\infty}$  concept at each vertex  $w_i$  to perform smooth lateral transitions which is important to provide comfort riding. This is achieved using certain weighting functions  $W_e^{(1)}$  and  $W_u^{(1)} \forall i$ .

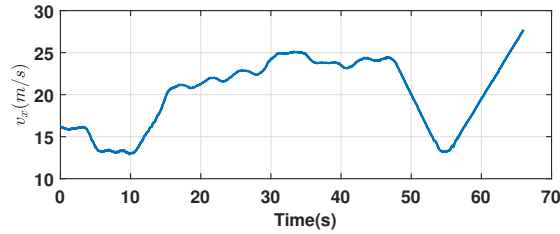


FIGURE 6 Simulation: Parameter-varying longitudinal speed  $v_x$  (m/s)

- LTI controllers  $K_i^{(2)}$  are designed separately using LTI/ $\mathcal{H}_\infty$  concept at each vertex  $w_i$  to perform fast lateral transitions to handle the vehicle when facing aggressive maneuvers and lateral oscillations. The chosen weighting functions are  $W_e^{(2)}$  and  $W_u^{(2)} \forall i$ .

### 6.3 Design the LPV-YK Control Structure

The following steps are done to design the LPV-YK control shown in Fig. 4:

- According to the method explained in Section 4 and **Theorem 1**, the LPV polytopic-based state-feedback controller  $F_g(\rho)$ , and the LTI state-feedback controllers  $F_{k,i}^{(0)}, \forall i \in \llbracket 1, 4 \rrbracket$ , can be designed using an LMI-based state-feedback approach (pole-placement constraints or Linear Quadratic Regulator).
- The state-space representations of  $M(\rho)$ ,  $N(\rho)$ ,  $U^{(0)}(\rho)$  and  $V^{(0)}(\rho)$  are computed as illustrated in Section 5.1, and  $Q^{(j)}(\rho, \gamma)$  ( $j \in \{1, 2\}$ ) is obtained from (20).

**Remark 2.** All the LPV systems  $V^{(0)-1}(\rho)$ ,  $U^{(0)}(\rho)$ ,  $N(\rho)$ ,  $M(\rho)$ , and  $Q^{(j)}(\rho)$  ( $\forall j$ ) are implemented in their state-space representations i.e. each LPV system is self-scheduled according to the change of the varying parameter  $\rho$ .

Simultaneously, to switch between LPV controllers, the switching signals  $\gamma_j$ 's are used to choose the LPV-YK parameter  $Q^{(j)}(\rho)$  that corresponds to the LPV controller  $K^{(j)}(\rho)$ . For more illustration, to switch from  $K^{(1)}(\rho)$  to  $K^{(2)}(\rho)$ , we assign  $\gamma_1 = 0$  and  $\gamma_2 = 1$ .

Here, the interpolating signal  $\gamma(t)$  is a vector of dimension two  $[\gamma_1(t), \gamma_2(t)]$ , where each  $\gamma_j$  multiplies its corresponding  $Q^{(j)}(\rho)$ . In this example, and based on an experimental experience,  $\gamma_2(t)$  is chosen to vary according to the demanded control tasks. Linear relations are proposed between different variables as follows:

- if  $\theta_e \leq 0.1$ ,  $\gamma_2(t) = \text{sat}(-y_L + 1.4 + 0.1\delta, [0, 1])$
- if  $\theta_e > 0.1$ ,  $\gamma_2(t) = \text{sat}(-0.7y_e + 1.4, [0, 1])$
- $\gamma_1(t) = 1 - \gamma_2(t)$

where  $\theta_e$  and  $y_e$  represent the heading and lateral errors between the vehicle and the current point on the reference path, respectively.  $\delta$  is the steering speed, and  $y_L$  is the lateral error at a look-ahead distance  $L$ <sup>42</sup>.

### 6.4 Simulation Results

The parameterized LPV-YK controller  $\tilde{K}(\rho, \gamma)$  is structured as shown in Fig. 4 and simulated on a nonlinear full car model designed for a Renault ZOE vehicle. The simulation is done using a part of a real trajectory map (*Satory*) where its coordinates are obtained from a pre-recorded map using a positioning system mounted on a real vehicle. The real vehicle speed from this recording is multiplied by 1.7 gain and used as a speed profile reference, to test the controllers within critical high speeds.

A scenario is chosen to cover several lateral tasks and critical situations as follows: 1) the vehicle is required to start its Autonomous Driving (AD) with a large lateral error ( $y_e > 2$  m); 2) When  $t \in [10, 40]$ s, the vehicle performs four successive turns at a high speed ( $v_x > 20$  m/s); 3) When  $t \in [40, 50]$ s, the vehicle is subjected to some sensor noises (due to real measurements) on a straight stretch; and finally 4) An obstacle is detected when  $t \in [50, 60]$ s, the navigation modifies the trajectory suddenly as two successive lateral steps (each one of 3 m), aiming to avoid a collision.

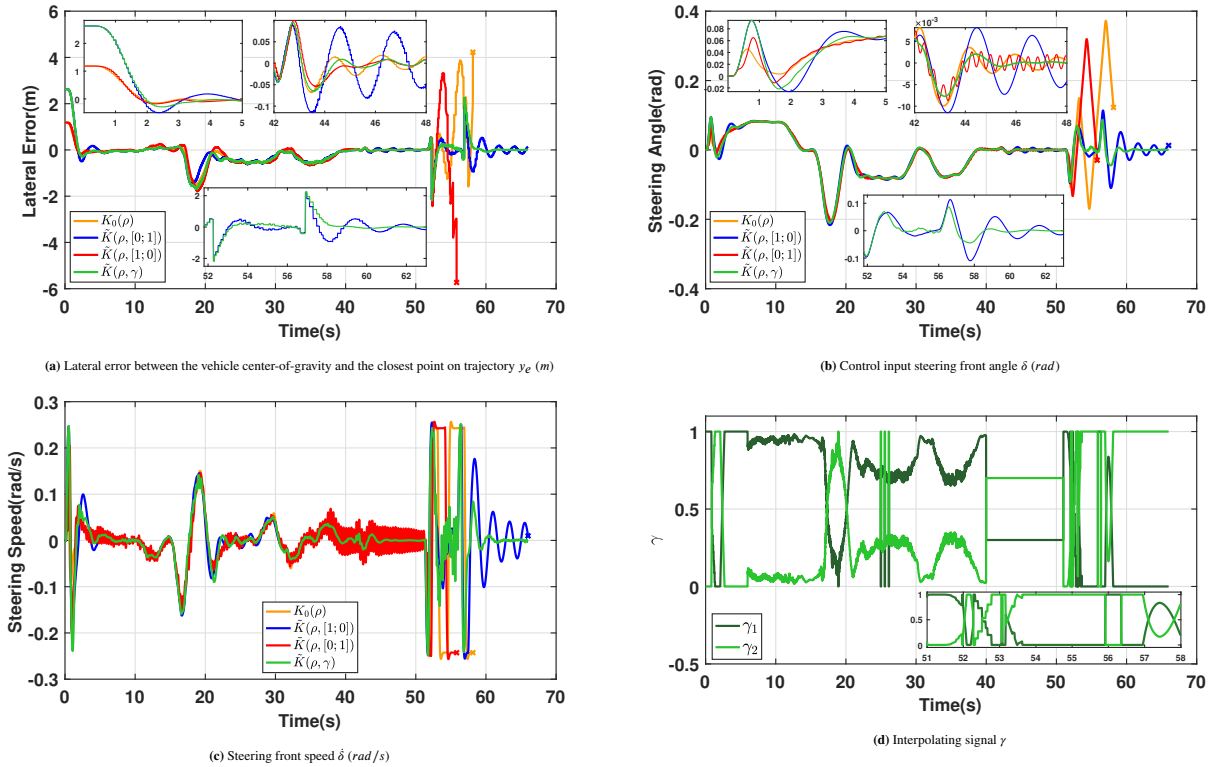


FIGURE 7 Simulation results

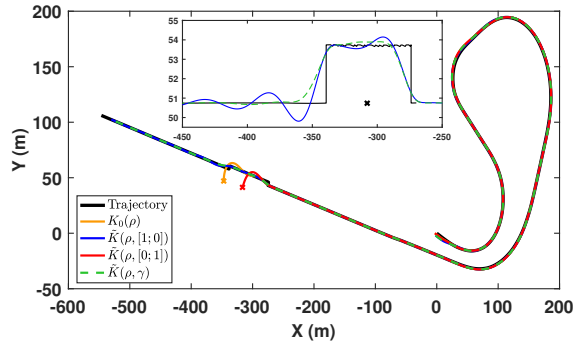


FIGURE 8 Simulation: Planned and controlled trajectories

The scenario is tested with different controllers:  $\tilde{K}(\rho, [0, 0]) \equiv K^{(0)}(\rho)$  (the nominal high robust controller),  $\tilde{K}(\rho, [1, 0]) \equiv K^{(1)}(\rho)$  (smooth tracker),  $\tilde{K}(\rho, [0, 1]) \equiv K^{(2)}(\rho)$  (aggressive tracker), and our proposed controller  $\tilde{K}(\rho, \gamma)$  with  $\gamma = [\gamma_1, \gamma_2]$  varies in real-time. Fig. 6 shows the speed profile for all the tests. Fig. 7a depicts the lateral error from the reference trajectory to the vehicle Center of Gravity (CoG), and the steering control input is shown in Fig. 7b. Fig. 7c represents the steering speed which reflects the driving comfort. Fig. 7d shows the evolution of the interpolating signal  $\gamma$  for  $\tilde{K}(\rho, \gamma)$ , and Fig. 8 shows the (X-Y) coordinates of the reference trajectory and the vehicle positioning response of the different tested controllers. The sub-figures in Figs. 7 and 8 show some zoomed results over time.

At  $t = 0s$ , it is shown in Fig. 7a that not all the tested controllers are activated to start at high lateral error ( $y_e > 2.5m$ ), since both controllers  $K^{(0)}(\rho)$  and  $\tilde{K}(\rho, [0, 1])$  can't deal with large lateral errors (observed from pre-testing). On the other hand,  $\tilde{K}(\rho, [1, 0])$  and  $\tilde{K}(\rho, \gamma)$  perform better with the initial high lateral error, where  $\tilde{K}(\rho, \gamma)$  shows a lower overshoot (see Fig. 7a when  $t \in [2, 5]s$ ) with a smoother steering action (see Fig. 7b when  $t \in [2, 4]s$ ). During the four successive turns, the four



tested controllers have almost similar tracking performance (check Fig. 7a), where there exists low steering noises using the fast controller  $\tilde{K}(\rho, [0, 1])$  as shown in Fig. 7c.

When  $t \in [42, 48]s$  (on the straight highway), Fig. 7a shows that the slow controllers ( $K^{(0)}(\rho)$ ,  $\tilde{K}(\rho, [1, 0])$ ) have lateral oscillations due to actuator limitations (for smoothness). On the other hand, the fast controller  $\tilde{K}(\rho, [0, 1])$  could handle the vehicle, but demanding more steering effort with noises (see Fig. 7c when  $t \in [42, 48]s$ ). However, due to the use of the steering speed in the proposed equations of  $\gamma_2$ ,  $\gamma$  changes to  $[0.3, 0.7]$ , and  $\tilde{K}(\rho, \gamma)$  achieves a perfect trade-off between decreasing the lateral oscillations (in Fig. 7a) and relaxing the steering action (in Fig. 7b and 7c).

Finally, it is clear in Fig. 8 that both  $K^{(0)}(\rho)$  and  $\tilde{K}(\rho, [0, 1])$  could not perform a fast double lane-change to overcome an obstacle (represented as "x"). Although the smooth controller  $\tilde{K}(\rho, [1, 0])$  could succeed in performing it, however, the vehicle performs high lateral oscillations. On the other hand,  $\tilde{K}(\rho, \gamma)$  shows better performance without any lateral overshoots (see Fig. 7a when  $t \in [52, 62]s$ ) and with a very smooth and optimized steering action (see Fig. 7b and 7c when  $t \in [52, 62]s$ ). Thanks to the variations of  $\gamma$  which reflects the needed lateral task to the proposed parameterized controller  $\tilde{K}(\rho, \gamma)$ , obtaining a combination between the designed performances.

Table 1 summarizes the conclusions behind the simulation results. Each of the controllers  $K^{(0)}(\rho)$ ,  $K^{(1)}(\rho)$ , and  $K^{(2)}(\rho)$  has some advantages and disadvantages. Generally speaking,  $K^{(0)}(\rho)$  has shown high robustness, however it deteriorates its tracking accuracy. In addition,  $K^{(1)}(\rho)$  achieves good tracking performance, while it is not capable to handle the vehicle at high lateral accelerations. Moreover,  $K^{(2)}(\rho)$  is designed to handle high lateral accelerations which make it more sensitive to noises at high frequencies. Therefore, the solution is to use all the controllers, where each one is used in its preferred situation, which is achieved using the proposed LPV-YK controller  $\tilde{K}(\rho, \gamma)$ . Notice that  $\tilde{K}(\rho, \gamma)$  hasn't shown any performance deterioration in all driving situations.

**TABLE 1** Overview of the tested controllers in simulation

Controller	Value of interpolating vector $\gamma$	Control objective	Advantages	Disadvantages
$\tilde{K}(\rho, [0, 0]) \equiv K^{(0)}(\rho)$	[0,0]	Highly robust	High noise rejection due to bad environment conditions, sensor faults, etc.	Inaccurate tracking performance and conservative
$\tilde{K}(\rho, [1, 0]) \equiv K^{(1)}(\rho)$	[1,0]	Smooth tracker	Good tracking performance with smooth steering	Oscillatory and cannot perform well at high lateral accelerations
$\tilde{K}(\rho, [0, 1]) \equiv K^{(2)}(\rho)$	[0,1]	Aggressive tracker	Fast tracking performance and could achieve high lateral accelerations	Too sensitive to noises
$\tilde{K}(\rho, \gamma)$	variant as in Fig. 7d	Multiple objectives by varying the interpolating vector $\gamma$ .	All the mentioned advantages and even more by choosing the optimal combination of controllers by $\gamma$	No bad performance is observed

## 7 Experimental Results

The LPV-YK controller  $\tilde{K}(\rho, \gamma)$  is tested on a robotized electric Renault ZOE vehicle shown in Fig. 9. It is prepared for lateral and longitudinal controls by computer-controlled steering and pedal actuators. Vehicle speed and the global coordinates are measurable using GPS and IMU. Previously, we have tested a polytopic-based LPV controller  $K_1(\rho)$  which has been designed with the weights  $W_e^{(1)}$  and  $W_u^{(1)}$  (i.e. the same used to design  $\tilde{K}(\rho, [1, 0])$ ), and using the standard polytopic optimisation problem<sup>4</sup>. Notice that the interpolating signal vector  $\gamma$  is switched manually during the test. This section aims mainly to: 1) Compare both controllers  $K_1(\rho)$  and  $\tilde{K}(\rho, [1, 0])$ ; and 2) Observe the controller response when switching  $\gamma$  rapidly as a step.

The test is done in a part of *Satory* test-track shown in Fig. 10. This test-track is challenging concerning the bad road conditions and its inclinations. Fig. 11a shows the variation of the measured longitudinal speed in *Kph* which is considered to be coherent with respect to the road curvature. The switching signal between controllers is presented in Fig. 11b. The vehicle starts on a straight highway using the smooth controller  $\tilde{K}(\rho, [1, 0])$ . Then, it switches to the faster controller  $\tilde{K}(\rho, [0, 1])$  when approaching two successive maneuvers (at  $t = 20s$ ) aiming to achieve the lowest lateral error. After exiting the successive maneuvers, it switches again to the smooth controller  $\tilde{K}(\rho, [1, 0])$  (at  $t = 50s$ ) and enters a second maneuver to compare its performance to the previously tested polytopic LPV controller  $K_1(\rho)$ .



FIGURE 9 Renault ZOE automated vehicle

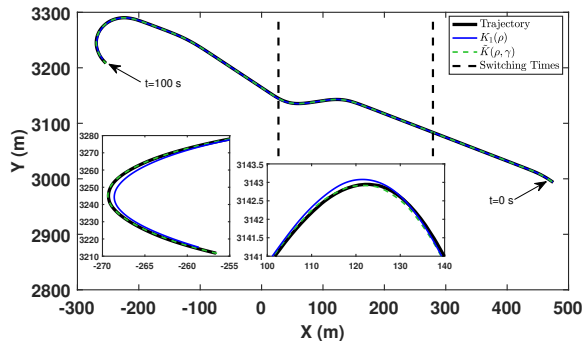


FIGURE 10 Experimental planned and controlled trajectories

Regarding Figs. 11c and 11d, it is clearly shown that the vehicle performance is not affected during the switching times (at  $t = 20s$  and  $t = 50s$ ) with negligible transient response. When  $t \in [20, 50]s$ ,  $\tilde{K}(\rho, [0, 1])$  achieves smaller lateral error compared to  $K_1(\rho)$  (see Fig. 11c), but with low steering noises as shown in Fig. 11d. Notice that these steering noises has been observed also in simulation section for  $\tilde{K}(\rho, [0, 1])$ . When  $t \in [65, 85]s$ ,  $\tilde{K}(\rho, [1, 0])$  shows lower lateral error during maneuvering compared to  $K_1(\rho)$ . This appears since the LPV-YK controller  $\tilde{K}(\rho, [1, 0])$  is less conservative than the polytopic LPV controller  $K_1(\rho)$ .

## 8 Conclusion

This work has proposed a new YK-based method to: 1) Design several gain-scheduled controllers based on interpolation of previously designed LTI controllers at the vertices of the polytopic region; 2) Interpolate between them to obtain various performances. An external signal vector is introduced to the parameter region, which can be used to incorporate any ad-hoc physically-based interpolation, without adding any conservatism to the design problem. As a result, the closed-loop quadratic stability is guaranteed under arbitrary interpolating signal and arbitrary parameter-variations.

This approach improves the system performance, while dealing with various objectives and situations. An application to the autonomous vehicle lateral control is carried out. The simulation shows interesting results regarding the efficiency of the proposed method of providing high performance and ensuring safety at critical situations. In addition, experimental results are shown to validate its real performance by testing the approach on a real Renault ZOE vehicle.

Finally, notice that the LPV-YK control structure facilitates adding any new controller, by introducing its corresponding LPV-YK parameter to the YK configuration (as shown in Fig. 2), without recalling all the control design procedure. This enhances real applications, such as in industries, where the systems are subjected to frequent instrumentation changes such as autonomous vehicles. In addition, several applications can benefit from the proposed approach, specifically the ones that change dynamics or need to perform different closed-loop performances having wide range of parameter variations.

As future work, an interest appears to study the optimal choice of  $\gamma$ , and how to find always the best combination of a larger set of controllers, which will improve more the presented work.

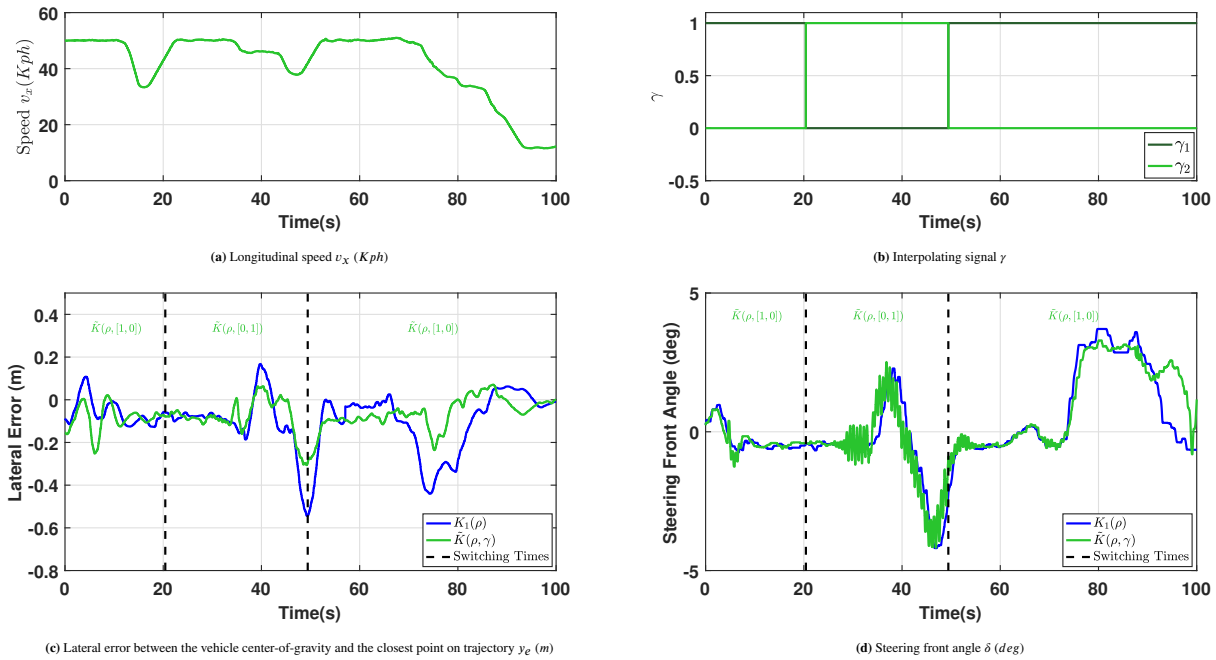


FIGURE 11 Experimental results

## References

1. Pacejka H. *Tire and vehicle dynamics*. Elsevier . 2005.
2. Rajamani R. *Vehicle dynamics and control*. New York, USA: Springer Science & Business Media . 2011.
3. Mariano R, Scalzi S, Netto M. Nested PID steering control for lane keeping in autonomous vehicles. *Control Engineering Practice* 2011; 19(12): pp 1459-1467. doi: 10.1016/j.conengprac.2011.08.005
4. Packard A. Gain scheduling via linear fractional transformations. *Systems & Control Letters* 1994; 22(2): 79-92. doi: [https://doi.org/10.1016/0167-6911\(94\)90102-3](https://doi.org/10.1016/0167-6911(94)90102-3)
5. Rugh W, Shamma J. Research on Gain Scheduling. *Automatica* 2000; 36: 1401-1425. doi: 10.1016/S0005-1098(00)00058-3
6. Hoffmann C, Werner H. A Survey of Linear Parameter-Varying Control Applications Validated by Experiments or High-Fidelity Simulations. *IEEE Transactions on Control Systems Technology* 2015; 23(2): 416-433. doi: 10.1109/TCST.2014.2327584
7. Apkarian P, Gahinet P. A convex characterization of gain-scheduled  $H_\infty$  controllers. *IEEE Transactions on Automatic Control* 1995; 40(5): 853-864. doi: 10.1109/9.384219
8. Apkarian P, Gahinet P, Becker G. Self-scheduled H control of linear parameter-varying systems: a design example. *Automatica* 1995; 31(9): 1251-1261.
9. Fen Wu , Xin Hua Yang , Packard A, Becker G. Induced  $\mathcal{L}_2$  norm control for LPV system with bounded parameter variation rates. *Proceedings of 1995 American Control Conference - ACC'95* 1995; 3: 2379-2383 vol.3. doi: 10.1109/ACC.1995.531398
10. Sename O, Gaspar P, Bokor (Eds) J. *Robust control and linear parameter varying approaches: application to vehicle dynamics*. 437. Springer, LNCIS . 2013.
11. Gáspár P, Szabó Z, Bokor J, Németh B. *Robust Control Design for Active Driver Assistance Systems: A Linear-Parameter-Varying Approach*. Springer International Publishing . 2017.

12. Mohammadpour J, Scherer CW. *Control of Linear Parameter Varying Systems with Applications*. Springer-Verlag New York . 2012.
13. Li P, Nguyen AT, Du H, Wang Y, Zhang H. Polytopic LPV approaches for intelligent automotive systems: State of the art and future challenges. *Mechanical Systems and Signal Processing* 2021; 161: 107931. doi: <https://doi.org/10.1016/j.ymsp.2021.107931>
14. Corno M, Panzani G, Roselli F, Giorelli M, Azzolini D, Savaresi SM. An LPV Approach to Autonomous Vehicle Path Tracking in the Presence of Steering Actuation Nonlinearities. *IEEE Transactions on Control Systems Technology* 2020: 1-9. doi: 10.1109/TCST.2020.3006123
15. Atoui H, Milanés V, Sename O, Martinez JJ. Design And Experimental Validation Of A Lateral LPV Control Of Autonomous Vehicles. *IEEE 23rd International Conference on Intelligent Transportation Systems (ITSC)* 2020: 1-6. doi: 10.1109/ITSC45102.2020.9294459
16. Atoui H, Sename O, Alcalá E, Puig V. Parameter Varying Approach For A Combined (Kinematic + Dynamic) Model Of Autonomous Vehicles\*\*Institute of Engineering Univ. Grenoble Alpes. *IFAC-PapersOnLine* 2020; 53(2): 15071-15076. 21st IFAC World Congressdoi: <https://doi.org/10.1016/j.ifacol.2020.12.2028>
17. Kapsalis D, Sename O, Milanés V, Molina JJ. A reduced LPV polytopic look-ahead steering controller for autonomous vehicles. *Control Engineering Practice* 2022; 129: 105360. doi: <https://doi.org/10.1016/j.conengprac.2022.105360>
18. Do AL, Fauvel F. LPV approach for collision avoidance: Controller design and experiments. *Control Engineering Practice* 2021; 113: 104856. doi: <https://doi.org/10.1016/j.conengprac.2021.104856>
19. Dániel Fényes BN, Gáspár P. Design of LPV control for autonomous vehicles using the contributions of big data analysis. *International Journal of Control* 2022; 95(7): 1802-1813. doi: 10.1080/00207179.2021.1876922
20. Lu B, Wu F. Switching LPV control designs using multiple parameter-dependent Lyapunov functions. *Automatica* 2004; 40: 1973-1980. doi: 10.1016/j.automatica.2004.06.011
21. Bianchi F, Peña R. Interpolation for gain-scheduled control with guarantees. *Automatica* 2011; 47(1): 239–243.
22. Niemann H. Dual Youla parameterisation. *IEE Proceedings - Control Theory and Applications* 2003; 150(5): 493-. doi: 10.1049/ip-cta:20030685
23. Rasmussen B, Chang Y. Stable Controller Interpolation and Controller Switching for LPV Systems. *Journal of Dynamic Systems Measurement and Control-transactions of The Asme - J DYN SYST MEAS CONTR* 2010; 132. doi: 10.1115/1.4000075
24. Blanchini F, Casagrande D, Miani S, Viaro U. Stable LPV Realization of Parametric Transfer Functions and Its Application to Gain-Scheduling Control Design. *IEEE Transactions on Automatic Control* 2010; 55(10): 2271-2281. doi: 10.1109/TAC.2010.2044259
25. Xie W, Eisaka T. Design of LPV control systems based on Youla parameterisation. *IEE Proceedings - Control Theory and Applications* 2004; 151(4): 465-472. doi: 10.1049/ip-cta:20040513
26. Atoui H, Sename O, Milanés V, Martínez Molina JJ. Advanced LPV-YK Control Design with Experimental Validation on Autonomous Vehicles. submitted to *Automatica*; 2022.
27. Hespanha J, Morse AS. Switching between stabilizing controllers. *Automatica* 2002; 38(11): 1905–1917.
28. Stoustrup J, Niemann H. Starting up unstable multivariable controllers safely. *Proceedings of the 36th IEEE Conference on Decision and Control* 1997; 2: 1437-1438 vol.2.
29. Tay T, Moore J, Mareels I. *High performance control*. Springer Science & Business Media . 1997.
30. Stoustrup J. Plug&play control: Control technology towards new challenges. *European Journal of Control* 2009: 311-330.
31. Atoui H, Sename O, Milanés V, Martínez JJ. Interpolation of Multi-LPV Control Systems Based on Youla-Kucera Parameterization. *Automatica* 2021; 134: 109963. doi: <https://doi.org/10.1016/j.automatica.2021.109963>

32. Mahtout I, Navas F, Milanés V, Nashashibi F. Advances in Youla-Kucera parametrization: A Review. *Annual Reviews in Control* 2020. doi: 10.1016/j.arcontrol.2020.04.015
33. Landau I. On the use of Youla-Kucera parametrization in adaptive active noise and vibration control-A review. *International Journal of Control* 2018: 1-25. doi: 10.1080/00207179.2018.1548773
34. Mahtout I, Navas F, Gonzalez D, Milanés V, Nashashibi F. Youla-Kucera Based Lateral Controller for Autonomous Vehicle. *21st International Conference on Intelligent Transportation Systems (ITSC)* 2018: 3281-3286. doi: 10.1109/ITSC.2018.8569779
35. Bei Lu , Fen Wu , SungWan Kim . Switching LPV control of an F-16 aircraft via controller state reset. *IEEE Transactions on Control Systems Technology* 2006; 14(2): 267-277.
36. He T, Zhu G, Swei S. Smooth Switching LPV Dynamic Output-feedback Control. *International Journal of Control, Automation and Systems* 2019; 18. doi: 10.1007/s12555-019-0088-3
37. Hanifzadegan M, Nagamune R. Smooth switching LPV controller design for LPV systems. *Autom.* 2014; 50: 1481-1488.
38. Atoui H, Sename O, Milanés V, Martínez-Molina JJ. Toward switching/interpolating LPV control: A review. *Annual Reviews in Control* 2022; 54: 49-67. doi: <https://doi.org/10.1016/j.arcontrol.2022.07.002>
39. Atoui H, Sename O, Milanés V, Martínez JJ. LPV-Based Autonomous Vehicle Lateral Controllers: A Comparative Analysis. *IEEE Transactions on Intelligent Transportation Systems* 2021: 1–12. doi: 10.1109/tits.2021.3125771
40. Vidyasagar M. Control system synthesis: a factorization approach, part II. *Synthesis lectures on control and mechatronics* 2011; 2(1): 1–227.
41. Angelis G. *System Analysis, Modelling and Control with Polytopic Linear Models*. PhD thesis. Department of Mechanical Engineering, 2001
42. Kosecka J, Blasi R, Taylor CJ, Malik J. Vision-based lateral control of vehicles. *Proceedings of Conference on Intelligent Transportation Systems* 1997: 900-905.

## Author Biography



**Hussam Atoui** received the B.Sc. degree in mechanical engineering from Lebanese University, the M.Sc. degree in Automatic Control from Grenoble-Alpes University in 2019, and the Ph.D. degree in automatic control engineering from Grenoble-Alpes University in 2022 in a joint research between Gipsa-lab Renault SAS. Then, he was awarded "*The Best Thesis Award*" from GDR-MACS in 2023. Since 2022, he is with the Driving Assistance Research (DAR) Team at Valeo, France. He is the author or a coauthor of more than 10 refereed publications in international journals and conference proceedings; and more than 5 industrial patents. His research interests concern switching control, youla parameterization, robust control, LPV control, and mainly control and motion planning of autonomous vehicles.



**Olivier Sename** received a Ph.D. degree from Ecole Centrale Nantes in 1994. He is now Professor at the Institut Polytechnique de Grenoble within GIPSA-lab. His main research interests include Linear Parameter Varying systems and automotive applications. He is the (co-)author of 2 books, 60 international journal papers, and more than 200 international conference papers. He was the General Chair of the IFAC Joint Conference SSSC-TDS-FDA 2013, of the 1st IFAC Workshop on Linear Parameter Varying Systems 2015 and he was the IPC Chair of the 2nd IFAC Workshop LPVS 2018. He has led several industrial (Renault, Volvo Trucks, JTEKT, Delphi) and international (Mexico, Italy, Hungary) collaboration projects. He has supervised 32 Ph.D. students.



**Vicente Milanés** received his Ph.D. degree in electronic engineering from University of Alcalá, Madrid, Spain, in 2010. He was with the AUTOPIA program at the Center for Automation and Robotics (UPM-CSIC, Spain) from 2006 to 2011. Then, he was awarded with a two-years Fulbright fellowship at California PATH, UC Berkeley. In 2014, he joined the RITS team at INRIA, France. Since 2016, he is with the Research Department at Renault, France. He is the author or a coauthor of more than 120 refereed publications in international journals, book chapters, and conference proceedings; and more than 10 industrial patents. His research interests cover multiple aspects in the autonomous vehicle field.



**John J. Martinez** was born in Cali, Colombia. He received the B.Sc. degree in electrical engineering and the M.Sc. degree in automatic control from the Universidad del Valle, Cali, in 1997 and 2000, respectively, and the Ph.D. degree in automatic control from the Institut National Polytechnique de Grenoble, Grenoble, France, in 2005. He joined the Universidad Nacional de Colombia, Medellin, Colombia, as a Teacher Assistant, from 2001 to 2002. He was an Invited Visitor with the Centre for Complex Dynamic Systems and Control, The Newcastle University, Callaghan, NSW, Australia, in 2005, 2007, and 2009. He is currently an associate professor at Grenoble-INP and researcher at GIPSA-lab (Control System Department). His research interest is related to modeling and robust control of mechatronic systems (e.g. Polytopic system modeling, Linear Parameter-Varying systems, Switching control and Invariant-Set Theory for Fault-Tolerant Control and Robust Disturbance Estimation/Rejection), mostly in the following applications: Automotive vehicle dynamics Safety, Aerial vehicle dynamics, Wind turbines control, Physiologic-aware electric bikes and Anti-vibration systems.

